



TEKSTİL VE MÜHENDİS
(Journal of Textiles and Engineer)



<http://www.tekstilvemuhendis.org.tr>

Numerical Investigation of Thermal Regulation Inside Firefighter Protective Clothing

İtfaiyeci Kıyafeti İçerisindeki Isıl Düzenlemenin Sayısal İncelenmesi

Ersin ALPTEKİN, Mehmet Akif EZAN, Berkant Murat GÜL, Hüseyin KURT, Atıf Canbek EZAN
Dokuz Eylül University, Department of Mechanical Engineering, İzmir, Turkey

Online Erişime Açıldığı Tarih (Available online): 30 Haziran 2017 (30 June 2017)

Bu makaleye atıf yapmak için (To cite this article):

Ersin ALPTEKİN, Mehmet Akif EZAN, Berkant Murat GÜL, Hüseyin KURT, Atıf Canbek EZAN
(2017): Numerical Investigation of Thermal Regulation Inside Firefighter Protective Clothing, Tekstil
ve Mühendis, 24: 106, 94-100.

For online version of the article: <https://doi.org/10.7216/1300759920172410606>



Arastırma Makalesi / Research Article

NUMERICAL INVESTIGATION OF THERMAL REGULATION INSIDE FIREFIGHTER PROTECTIVE CLOTHING

Ersin ALPTEKİN
Mehmet Akif EZAN*
Berkant Murat GÜL
Hüseyin KURT
Atf Canbek EZAN

Dokuz Eylül University, Department of Mechanical Engineering, Izmir, Turkey

Gönderilme Tarihi / Received: 03.01.2017

Kabul Tarihi / Accepted: 31.05.2017

ABSTRACT: Phase change materials (PCMs) are widely used in heating and cooling applications to reduce the mismatch between the energy production and the demand. PCMs can also be incorporated into the thermal systems to maintain a constant temperature and conduce to increase the thermal comfort. Unlike any human-made thermal system, the thermal comfort of the human body is more crucial since a possible damage may not be recovered. In this study, PCM layers are incorporated into the textile fabric to increase the thermal comfort of a firefighter and protect the skin layers from the thermal burn due to overheating. A transient one-dimensional numerical model is developed in the ANSYS-FLUENT software. The effect of blood perfusion inside skin layers is simulated as an energy source term and defined into the software using user-defined-function (UDF). The validity of the source term implementation into ANSYS-FLUENT is proven by reproducing a reduced model from the literature. The predicted time-wise variations of the temperature of the body layers are compared with the ones which are taken from the literature. After the validation procedure, the usage of PCM inside a firefighter protective clothing is numerically investigated by varying the thermal boundary conditions acting on the coating. Results depict that, for the longest fire exposure duration the 1st-degree burn is effective for a depth of 5.29 mm and the 3rd-degree burn is observed for a depth of 2.57 mm. Implementing the PCM inside the clothing inhibits the temperature rise in skin layers and improves the heat storage capacity of the fabric. In the current design and working conditions, firefighter protective clothing with 1 mm of PCM layer prevents the skin burn, even for the longest fire exposure scenario.

Keywords: Textile, phase change materials, numerical model, thermal protection, thermal burn

İTFAİYECİ KIYAFETİ İÇERİSİNDEKİ ISIL DÜZENLEMENİN SAYISAL İNCELENMESİ

ÖZET: Faz değişim malzemeleri (FDM) enerji üretimi ve talebi arasındaki uyumsuzluğu azaltmak amacıyla ısıtma ve soğutma uygulamalarında yaygın olarak kullanılmaktadır. FDM'ler ayrıca ısı sistemler içerisine uygulanarak sabit sıcaklık sağlar ve ısı konforun artmasına vesile olurlar. İnsanoğlu tarafından üretilen tüm sistemlerden farklı olarak olası bir hasarın geri dönüşünün mümkün olmaması nedeniyle, insan vücudunun ısı konfor koşulları çok daha önemlidir. Bu çalışmada itfaiyecinin ısı konfor koşullarının artırılması ve aşırı ısınma kaynaklı deri hasarlarının engellenmesi amacıyla tekstil kumaşı tabakaları içerisine faz değişim malzemesi yerleştirilmiştir. ANSYS-FLUENT paket programında zamana bağlı 1-boyutlu bir sayısal model geliştirilmiştir. Deri katmanları içerisindeki kan dolaşımından kaynaklı ısı transferi etkisini programda tanımlamak için kullanıcı-tanımlı-fonksiyon (UDF) oluşturulmuş ve programa aktarılmıştır. ANSYS-FLUENT paket programı içerisine tanımlanan kaynak terimlerinin uygunluğunu test etmek için öncelikle literatürden alınan basitleştirilmiş bir problem tekrarlanmıştır. Deri katmanları içerisindeki zamana bağlı sıcaklık değişimleri literatürden alınan sonuçlarla karşılaştırılmıştır. Modelin doğrulanmasından sonra ise itfaiyeci kıyafeti içerisinde FDM kullanımı farklı ısı sınır koşulları için sayısal olarak incelenmiştir. En uzun süreli yangın etki durumunda 1. Derece ve 3. Derece yanık derinlikleri sırasıyla 5,29 mm ve 2,57 mm olarak belirlenmiştir. FDM'nin kumaş içerisine yerleştirilmesi malzemenin ısı depolama kapasitesini arttırmakta ve deri katmanlarının sıcaklık artışı engellemektedir. Mevcut tasarım ve çalışma koşullarında, 1 mm kalınlığında FDM içeren itfaiyeci kıyafetinin en uzun yangın etki senaryosunda dahi deri hasarını engellediği saptanmıştır.

Anahtar kelimeler: Tekstil, Faz değişim malzemeleri, Sayısal model, Isıl koruma, Isıl yanma

* Sorumlu Yazar/Corresponding Author: mehmet.ezan@deu.edu.tr

DOI: 10.7216/1300759920172410606, www.tekstilmuhendis.org.tr

1. INTRODUCTION

ASHRAE defines the human thermal comfort as the state of mind that expresses satisfaction with the environmental conditions [1]. Thermal comfort of the human body is related to the heat and mass transfer mechanisms between the skin and the environment. The heat can be moved through (or *from*) the surroundings by heat conduction, convection, radiation, and evaporation. The thermal comfort of a body could be maintained when the generated heat by the human metabolism is rejected through the surroundings. If there is a heat gain or loss beyond this thermal equilibrium, the person will feel discomfort. The body core temperature is almost constant even though the surrounding temperature varies significantly. Body temperature is controlled by blood flow inside the skin or the evaporating mechanism [1]. Heat-related illnesses (*hypothermia* or *hyperthermia*) may arise when the body temperature exposed extremely hot or cold environments.

Excessive heat or contact with chemical substances may cause thermal burns (or *injuries*) that result in the destruction of the human tissues on the outer layer of the skin. The threshold temperature for the thermal burn is 317 K [2]. At relatively low temperatures, such as 317 K, the thermal injury may occur for a long-term exposure (5 to 6 hours), but at higher temperatures, i.e. 327 K, destruction begins within seconds. In a recent work of the fire protection research foundation [3], it is stated that a significant number of thermal injuries occur when the energy stored within the protective clothing of firefighter and suddenly transferred to the firefighter. Storing the excessive heat inside the protective clothing and then release the stored heat without causing any damage to the firefighter is crucial to prevent the thermal injury.

Energy can be stored in a medium in two different ways: sensible and latent heat storage. Sensible heat storage is proportional to the heat capacity of the material and the temperature variation. In the case of protective clothing, to avoid the thermal injury, sensible storage is not a good option since the increasing temperature is a potential risk for the human body. Instead, excessive heat should be stored in the medium without causing a temperature increment. Phase change materials (PCMs), on the other hand, can store the excessive heat without causing a temperature increase in a long-term usage. PCMs store the thermal energy during the solid to liquid phase change (*melting*) and release the thermal energy during the reverse phase change process (*solidification*). The amount of stored energy within the PCM depends on the phase change enthalpy of the (*latent heat*) of the material. The materials that are proposed as PCMs have higher latent heat and constant phase temperature (*melting* or *solidification*) without sub-cooling effect. PCMs are commonly used in heating [4] and cooling applications [5] as a storage medium to reduce mismatch the energy supply and demand. As an instance, in a solar power plant, to provide a continuous (24 h) electricity generation throughout the day, heat can be stored in a PCM tank during the day time, in the form of latent heat, and the

stored thermal energy can be re-used at night hours. Recently, PCMs are also utilized as a thermal buffer to keep a system temperature within a pre-defined range. In buildings [6] or electronic devices [7], PCM layers are used to absorb the excessive heat so that the sudden variations are avoided. As a thermal buffer, PCMs are also incorporated in textile fabrics. PCM can be applied to textile material as layers or inside microcapsules to provide thermal regulation [8]. Mondal (2008) [9] states that the microencapsulated PCM technology in the textile structure was firstly used by NASA researchers in the early 1980s to provide an improved thermal protection in the fabrics of astronauts against sudden temperature changes in outer space.

Shin et al. (2005) [10] developed a thermo-regulating textile material by incorporating microencapsulated eicosane. Eicosane is covered by melamine - formaldehyde microcapsules which are prepared by in situ polymerizations. The thermal energy storage capacity of the proposed material is obtained in the range of 0.91 to 4.44 J/g depending on the mass fraction of the eicosane. However, it is also indicated that after five launderings the storage capacity of the treated fabric can be reduced more than half. Tong & Tong (2015) [11] developed a novel textile fabric for outdoor wear in cold weather absorbs solar energy during the daytime. It is proposed that the developed material can be used in life-saving military uniforms and performance sportswear. Li & Zhu (2004) [12] numerically investigated the heat and moisture transfer in a porous textile fabric. PCM is embedded inside the textile material to improve the energy storage capability. Numerical predictions are compared with the experimental measurements to validate the developed scheme. Shaid et al. (2015) [13] developed a firefighter garment which can provide improved thermal protection to prevent heat loss. They claimed that as a standard approach aerogel is used in high heat protection. Aerogel not only blocks the incoming heat flux through the body but also restricts the heat loss from the body surface. Consequently, the wearer suffers from an increase in body temperature [13]. The embedded PCM layer improves the thermal protection and comfort. Hu et al. (2013) [2] incorporated PCM in a firefighter protective clothing. The influence of PCM position in the fabric is revealed under constant heat flux condition. The time-wise variation of thermal damage is also obtained. The results depict that placing the PCM between the waterproof layer and the inner layer is the most appropriate design.

In the current study, a one-dimensional numerical model is developed to predict combined heat transfer within the layers of textile fabric and tissue. 1 mm PCM layer is placed inside the fabric to examine the influence of the PCM on the thermal comfort of the firefighter. Unlike the previous papers in the literature, thermal boundary condition on the protective cloth is defined as a function of time. A cyclic boundary condition is defined in such a way that the firefighter protective clothing is exposed to the flame for a certain duration of $\Delta t_{exposure}$ and then be far away from the fire for $\Delta t_{protection}$.

2. MATERIAL & METHOD

2.1. Definition of the Problem

Coupled transient heat transfer inside multi-layer firefighter protective clothing (FPC) and skin layers are numerically simulated. Figure 1 shows the layers of the fabric and the skin. There is a total of five layers in the FPC and skin consist of three layers. From left to right the layers of FPC are outer shell ($L_{os} = 0.7$ mm), waterproof ($L_{wp} = 1.12$ mm), PCM ($L_{PCM} = 1$ mm), inner layer ($L_{il} = 0.95$ mm) and air gap ($L_{ag} = 6.35$ mm). The skin layers, on the other hand, are epidermis ($L_{ed} = 0.08$ mm), dermis ($L_{ed} = 2.0$ mm) and the subcutaneous ($L_{sub} = 10.0$ mm).

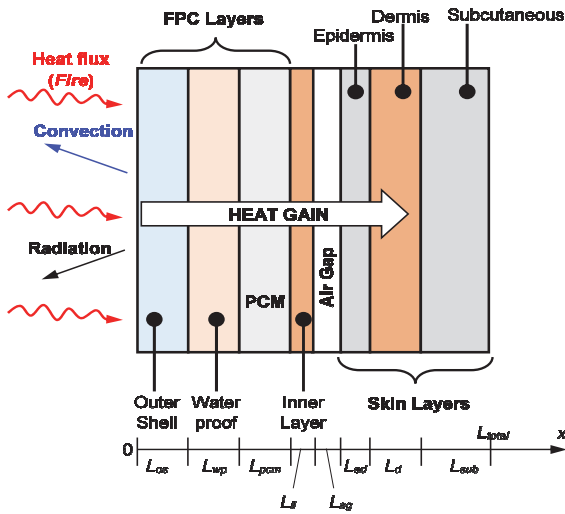


Figure 1. One dimensional mathematical model

On the outer layer of the FPC, there is a time-dependent and coupled boundary conditions. The mathematical expression of the boundary condition on outer surface is given as follows,

$$-k \frac{\partial T}{\partial x} \Big|_{x=0} = q''_{fire} - \varepsilon \sigma (T_{x=0}^4 - T_{surr}^4) - h(T_{x=0} - T_{\infty}) \quad (1)$$

where q''_{fire} is the average heat flux of a flame. $T_{x=0}$, T_{surr} and T_{∞} are the outer surface temperature, surrounding temperature and the ambient temperature, respectively. In the current analysis, q''_{fire} is assumed to be 2.5 kW per unit area [14]. To simulate the variable boundary condition on the external surface of the FPC, q''_{fire} , T_{surr} and T_{∞} are defined as time-dependent. On the inner face of the tissue ($x = L_{total}$), on the other hand, constant temperature is set,

$$T(x = L) = T_{core} \quad (2)$$

where T_{core} is the body core temperature and set to be 310 K [2]. Inside the skin layers, the heat transfer is quite complicated. In the current model, Pennes's approach [15] is followed to simulate the heat transfer between the flowing blood and the surrounding tissue [16]. Pennes defined the rate of heat transfer from the blood as a volumetric heat source (or sink) term,

$$\dot{q}_p = \omega \rho_{blood} c_{blood} (T_{core} - T) \quad (3)$$

ω is the volumetric blood flow rate per unit volume of tissue and known as perfusion rate. ρ_{blood} ($= 1060$ kg/m³) and c_{blood} ($= 3770$ J/kgK) are the density and specific heat of the blood, respectively. Blood perfusion $\omega = 0.00125$ m³/s/m³ is defined only in the dermis and subcutaneous layers.

2.2. Solution Method

One-dimensional mathematical model is developed in ANSYS-FLUENT software. The governing equation, which represents the heat diffusion inside the FPC, is as follows,

$$\frac{\partial}{\partial t} (\rho c T) = \frac{\partial}{\partial x} \left(k \frac{\partial T}{\partial x} \right) \quad (4)$$

For each layer, the density (ρ), specific heat (c) and the thermal conductivity (k) of the materials are defined according to the properties that are given in Table 1. For the PCM layer, apparent heat capacity approach of Morgan et al. (1978) [17] is used. In this method, the phase change is assumed to take place in a small temperature range, rather than a sudden change at a single temperature. The narrow temperature band bounded by the solidus temperature ($T_m - \delta T_m$) and liquidus temperature ($T_m + \delta T_m$). The solid/liquid phase change region is mostly called "mushy zone" [18]. The latent (heat of fusion) of the material is defined regarding the heat capacity of mushy zone,

$$c_{mushy} = \frac{h_{sf}}{2\delta T_m} + \frac{c_l + c_s}{2} \quad (5)$$

where h_{sf} is the latent heat of fusion. $2\delta T_m$ designates the mushy zone temperature range. Besides, c_l and c_s are the specific heat values of liquid and solid phases, respectively. In the current analyses to improve the accuracy of numerical prediction, a narrow mushy region is defined with $2\delta T_m = 1$ K. The melting temperature and heat of fusion of the PCM are $T_m = 351$ K and $h_{sf} = 267$ kJ/kg, respectively.

For epidermis and subcutaneous layers, an additional volumetric source (or sink) term should be defined to consider the heat transfer with perfusion flow,

$$\frac{\partial}{\partial t} (\rho c T) = \frac{\partial}{\partial x} \left(k \frac{\partial T}{\partial x} \right) + \dot{q}_p \quad (6)$$

The ANSYS-FLUENT software is used to resolve transient heat transfer inside the computational domain. A subroutine (User-Defined-Function - UDF) is coded in C++ language to implement the perfusion flow term (Eq. 3) into the energy balance equation (Eq. 6). An external profile file is also imported into the software to define a cyclic boundary condition on the outer surface of the FPC. The computational domain is divided into 50000 control volumes, and the time step size is selected to be 0.01 s. For each time step, the absolute residual of the energy equation is reduced below 1E-8 to minimize the numerical errors.

Table 1. Thermo-physical properties of layers [2]

Layer	ρ (kg/m ³)	c (J/kgK)	k (W/mK)
Outer Shell	286	1005	0.08
Waterproof	179.4	1940	0.037
PCM	2000	1100	0.65
Inner Layer	220	1300	0.052
Air gap	1.18	1005	0.026
Epidermis	1200	3600	0.24
Dermis	1200	3300	0.45
Subcutaneous	1000	2500	0.18

2.3. Validation of the Method

The numerical work of Ref [19] is reproduced to assess the validity of the current method. They have considered one-dimensional transient heat transfer inside skin layers. Initially, there is a linear temperature variation inside the domain between 34°C and 35°C. The outer surface of the skin is raised to 90°C. Figure 2 compares the length-wise temperature distributions and time-wise variation of threshold/3rd-degree burn. In Figure 2(a) the dashed lines represent the results of reference paper and the solid ones are the current predictions. It is clear that there is a small discrepancy between the current results and the reference within the range of 3 mm to 5 mm. As mentioned before, in the reference work, Jiang et al. (2002) [19] assumed that initially there is linear temperature profile inside the domain. However, since the details of the initial pattern did not provide in the reference work, in the current analysis, the initial temperature variation is assumed to be uniform. The small discrepancy may arise owing to the difference between the initial conditions.

In Figure 2(b), the variations of threshold (1st-degree burn) and 3rd-degree burns are compared with the reference work. The thermal injury of skin starts when the temperature reaches above 44°C. The impact of the thermal burns, on the other hand, are classified regarding the dimensionless damage function, $\Omega(x, t)$. Takata (1974) [21] states that a first-degree burn (*threshold*),

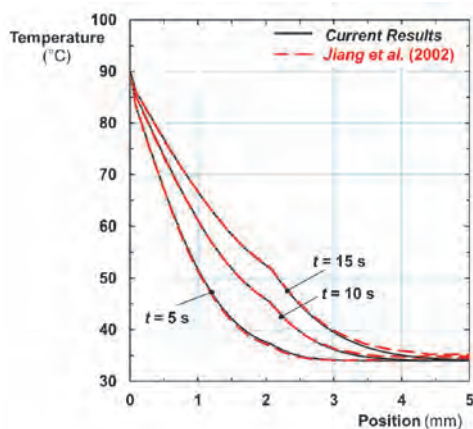
second-degree burn and third-degree burn corresponds to $\Omega = 0.53, 1.0$ and 10^4 , respectively. Henriques and Moritz (1947) [22] defines the burn damage as

$$\Omega(x, t) = \int_0^t P \exp(-\Delta E/RT(x, t)) dt \quad (7)$$

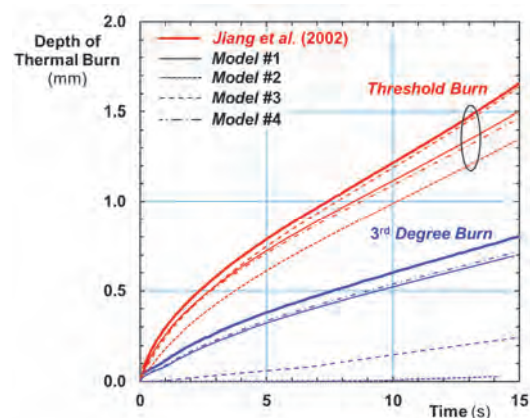
where ΔE is the activation energy (J/kmol), P is the frequency factor (1/s), and R is the ideal gas constant (J/kmolK). In the reference work [19], authors did not indicate the numerical values for ΔE and P . In the literature; several investigators have provided the activation energy and the frequency factor of the skin layers. Four commonly used model results are given in Table 2. It is clear that the values of ΔE and P vary in a wide range since the thickness of the skin layers differs person to person or even throughout a body. In the current work, the burn damage is calculated by using each of the four cases that are given in Table 2. An additional MATLAB function is developed to compute the thermal damage function (Ω) for each computational node. At the end of each time step, the temperature distribution is transferred from ANSYS-FLUENT to MATLAB code.

Table 2. Thermal damage parameters from different investigators

Model	Temperature Range (°C)	ΔE (J/kmol)	P (1/s)
#1 Henriques (1947) [22]	All T	6.27E8	3.1E98
#2 Fugitt (1955) [23]	$T \leq 55$ $T > 55$	6.27E8 2.96E8	3.1E98 5.0E45
#3 Stoll & Greene (1959) [24]	$T \leq 50$ $T > 50$	7.82E8 3.27E8	2.185E124 1.823E51
#4 Takata (1974) [20]	$T \leq 50$ $T > 50$	4.18E8 6.69E8	4.322E64 9.389E104



(a) Temperature distributions



(b) The evaluation of thermal burn

Figure 2. Validation of the numerical model

The time-wise variations of the thermal damage that are obtained from four different injury models are compared with the reference work in Figure 2(b). One can see that the activation energy and frequency factor of the material significantly alters the evaluation of thermal burn. Since the precise values are not provided in the reference work, it is not possible to perform a proper comparison regarding the thermal injury. However, it seems that the results obtained from Model #1 [22] are the closest one to the reference paper [19].

3. RESULTS & DISCUSSION

In the current analyses, a cyclic boundary condition is defined in such a way that the firefighter protective clothing is exposed to the flame for the duration of $\Delta t_{exposure}$ and then be far away from the fire for $\Delta t_{protection}$. To simulate the cyclic boundary condition on the surface of the fabric, the first terms in Eq. (1), q''_{fire} , is defined to be 2.5 kW/m^2 during the exposure duration. On the other hand, q''_{fire} is set to be zero during the protection time. That is, the stored energy inside the fabric or skin is released through the ambient in the protection period. The parameters that have been considered in the current numerical survey are listed in Table 3. Five fire exposure cases are examined by varying the ratio of exposure time to protection time as 1, 2, 3, 6 and 12. The current paper is motivated to investigate the merits of the implementation of PCM layer in protective clothing. Two sets of scenarios have been considered. In the first scenario, the reference clothing in which there is no PCM layer is simulated. In the second one, on the other hand, a model is generated which includes 1 mm of PCM layer between the waterproof and inner layer, as illustrated in Figure 1.

In Figures 3 and 4, the thermal response of a reference firefighter protective clothing, which does not include PCM, under varying boundary conditions are represented. Figure 3 shows the time-wise variation of the average skin layer, epidermis, dermis and

subcutaneous, temperatures. Here solid, dashed and dotted lines, respectively represent the epidermis, dermis, and subcutaneous layers. As it is expected, increasing the exposure time the average skin temperature raises. The influence of cyclic boundary condition becomes significant for higher exposure/protection durations, such as Cases 3, 4 and 5. When the boundary condition is switched from exposure to the protection mode, the curves become flat, so that step-like curves are observed. At the end of 900 s, the mean temperature of the epidermis layer reaches almost 80°C for Case 5. The average temperature of dermis layer, on the other hand, reaches nearly 75°C , at $t = 900 \text{ s}$. At $t = 675 \text{ s}$, the subcutaneous layer temperature reaches to 45°C , which is higher than the critical temperature for thermal injury. For Case 4, in which the exposure to protection-time ratio is six, the maximum temperatures for epidermis, dermis and subcutaneous layers are observed to be 73°C , 69°C , and 46°C , respectively. Decreasing the exposure period, i.e. Case 3 and 2, the maximum temperatures reduce significantly. In Case 3, the mean temperature of epidermis layer remains below 60°C . The dermis layer temperature is close to the epidermis layer, which is 57°C . For Case 2, the mean temperatures epidermis and dermis layers are 54°C and 52°C , respectively. In Case 1, the average temperatures of epidermis layer just reach to 45.6°C and 44.6°C at the end of 900 s, respectively. One can infer that the temperature difference between epidermis and dermis layers reduces as the protection time increases.

Table 3. Cyclic boundary conditions on the protective clothing

Case	Protection (s)	Exposure (s)	Ratio
#1	10	10	1.00
#2	10	20	2.00
#3	10	30	3.00
#4	10	60	6.00
#5	10	120	12.00

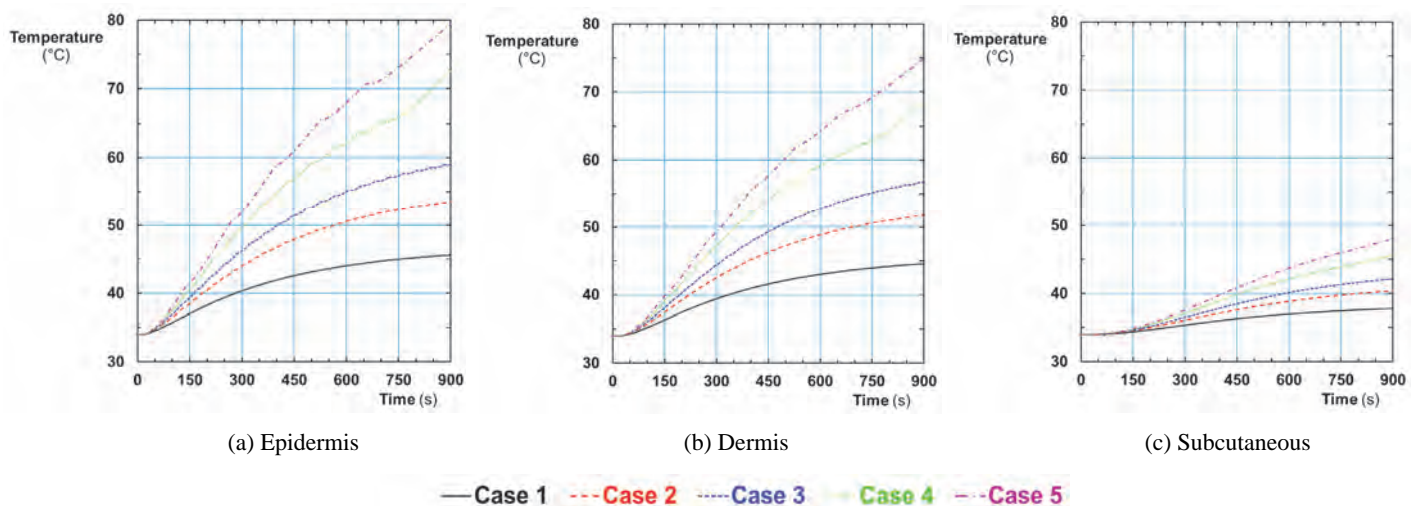


Figure 3. Time-wise variation of skin-layer temperatures – without PCM

Figure 4 illustrates the progress of the thermal burn. Here the solid lines represent the 1st-degree burn and dashed ones denote the 3rd-degree burn. The 1st degree and 3rd-degree burns are defined regarding the damage function, $\Omega(x, t)$, which is defined in Eq. (7). For Case 1 thermal damage is not observed since it corresponds to the shortest fire exposure duration. In Case 2, the exposure time is doubled to 20 s and the 1st-degree thermal burn takes place after 700 s. At the end of 900 s, the depth of burn reaches to 1.23 mm. In Case 3, on the other hand, the thermal burn starts earlier stages of the process, at $t = 500$ s and becomes effective in a depth of 2.93 mm. In Case 4, 1st-degree burn penetrates into deeper layers of the skin. The starting time of thermal burn is 375 s, and the maximum depth is 4.46 mm. 3rd-degree burn is observed in Case 4 when the damage function (Ω) reaches up to 10^4 . 3rd-degree burn starts at $t = 786$ s, and at the end of 900 s, the depth of the burn is observed to be 1.22 mm. In Case 5, on the other hand, the 1st-degree and 3rd-degree burns appears quite earlier stages and causes deeper damages as it possess the longest exposure duration. 1st-degree burn starts at $t = 330$ s and penetrates into 5.29 mm. Besides, 3rd-degree damage occurs at $t = 600$ s and becomes effective on 2.57 mm.

Figure 5 represents the time-wise variations of skin layers for firefighter protective clothing, which includes 1 mm of PCM between the inner layer and waterproof. It is interesting to note that, the temperature of skin layers vary with time almost identically until $t = 600$ s. PCM inhibits temperature rise on the skin surface and maintains nearly constant temperature for 600 s in all cases. At the end of 600 s, for Case 5, which corresponds the highest fire exposure duration, the mean temperature values for epidermis and dermis layers starts to increase and at the end of 900 s temperatures reach up to 47°C and 45°C, respectively. Since the skin layer temperature remains below the critical temperature, 44°C, the thermal burn is not observed in the scenario in which PCM is used inside the firefighter protective clothing.

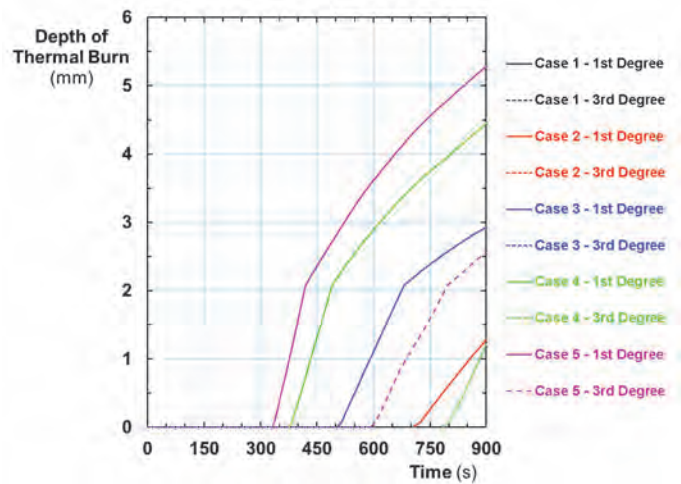
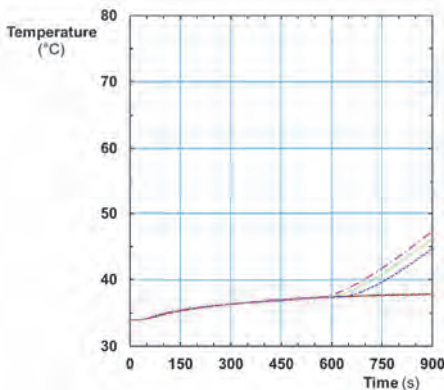


Figure 4. Evaluation of thermal burn – without PCM

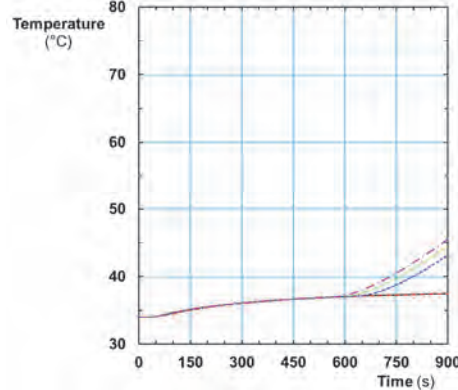
In Table 4, the results of two scenarios, the regular firefighter protective clothing and the one that includes PCM, are compared. Even for the worst case, Case 5, the PCM provides an improved protection to the firefighter and reduces the maximum skin temperature almost by 30°C. More importantly, implementing the PCM blocks the thermal injury.

Table 4. Comparative results for scenarios without PCM and with PCM

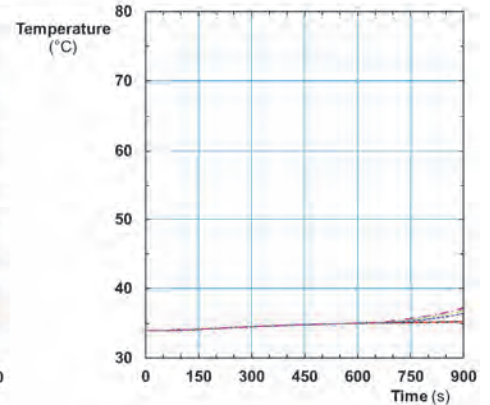
Case	w/o PCM			with PCM
	Max. Temp. (°C)	Depth of 1 st Degree Burn (mm)	Depth of 3 rd Degree Burn (mm)	Max. Temp. (°C)
#1	45.6	-	-	37.8
#2	53.6	1.28	-	37.8
#3	59.0	2.93	-	44.8
#4	72.6	4.46	1.22	46.3
#5	79.5	5.29	2.57	47.4



(a) Epidermis



(b) Dermis



(c) Subcutaneous

— Case 1 - - - Case 2 - · - Case 3 - · - Case 4 - - - Case 5

Figure 5. Time-wise variation of skin-layer temperatures – 1 mm PCM layer

4. CONCLUSION

This study focuses on the development of a numerical model in a commercial CFD code, ANSYS-FLUENT, to simulate the bio-heat problem for a firefighter protective clothing. Following results can be concluded:

- The proposed CFD model predicts the time-wise temperature variations and the progress of thermal damage are in accordance with the reference work,
- The depth of thermal burn increases for the extended fire exposure durations. The time of protection should be increased to provide excessive heat removal from the fabric.
- It is clear that PCM provides an improved protection. The maximum temperature of the skin layer remained close to the critical limit for thermal burn so that no injury is observed in PCM embedded firefighter protective clothing.

Further studies should be done to optimize the thickness, position and type of the PCM. The melting temperature of the PCM should be selected according to the maximum temperature values within the clothing.

REFERENCES

1. ASHRAE, F., (2013), *Fundamentals Handbook*, IP Edition.
2. Hu, Y., Huang, D., Qi, Z., He, S., Yang, H., & Zhang, H., (2013), *Modeling thermal insulation of firefighting protective clothing embedded with phase change material*, Heat and Mass Transfer, 49(4), 567-573.
3. NFPA, (2008), *Thermal Capacity of Fire Fighter Protective Clothing*, Fire Protection Research Foundation.
4. Kenisarin, M., & Mahkamov, K., (2007), *Solar energy storage using phase change materials*, Renewable and Sustainable Energy Reviews, 11(9), 1913-1965.
5. Ezan, M.A., & Ereğ, A., (2012), *Solidification and Melting Periods of an Ice-on-Coil Latent Heat Thermal Energy Storage System*, Journal of Heat Transfer, 134 (6), 062301.
6. Tyagi, V.V., Pandey, A.K., Buddhi, D., & Kothari, R., (2016), *Thermal performance assessment of encapsulated PCM based thermal management system to reduce peak energy demand in buildings*, Energy and Buildings, 117, 44-52.
7. Alshaer, W. G., Nada, S. A., Rady, M. A., Le Bot, C., & Del Barrio, E.P., (2015), *Numerical investigations of using carbon foam/PCM/ Nano carbon tubes composites in thermal management of electronic equipment*, Energy Conversion and Management, 89, 873-884.
8. Sarier N., & Onder E., (2012), *Organic phase change materials and their textile applications: an overview*, Thermochimica Acta, 540, 7-60.
9. Mondal, S., (2008), *Phase change materials for smart textiles – An overview*, Applied Thermal Engineering, 28, 1536-1550.
10. Shin, Y., Yoo, D. I., & Son, K., (2005), *Development of thermoregulating textile materials with microencapsulated phase change materials (PCM). II. Preparation and application of PCM microcapsules*, Journal of Applied Polymer Science, 96(6), 2005-2010.
11. Tong, W., Tong, A., (2015), *Thermal Modelling on Solar-Absorbing Metamaterial Microencapsulation of Phase Change Materials for Smart Textiles*, Journal of Textile Science & Engineering, 5:190.
12. Li, Y., & Zhu, Q., (2004), *A model of heat and moisture transfer in porous textiles with phase change materials*, Textile Research Journal, 74(5), 447-457.
13. Shaid, A., Wang, L., & Padhye, R., (2015), *The thermal protection and comfort properties of aerogel and PCM-coated fabric for firefighter garment*, Journal of Industrial Textiles, 1528083715610296.
14. Back, G., Beyler, C. L., DiNenno, P., & Tatem, P., (1994), *Wall incident heat flux distributions resulting from an adjacent fire*, Fire Safety Science, 4, 241-252.
15. Pennes, H., (1948), *Analysis of tissue and arterial blood temperatures in the resting human forearm*, Journal of Applied Physiology, 1(2), 93-122.
16. Bergman, T.L., Incropera, F.P., & Lavine, A.S., (2011), *Fundamentals of heat and mass transfer*, John Wiley & Sons.
17. Morgan, K., Lewis, R.W., & Zienkiewicz, O.C., (1978), *An improved algorithm for heat conduction problems with phase change*, International Journal for Numerical Methods in Engineering, 12(7), 1191-1195.
18. Voller, V.R., & Swaminathan, C.R., (1991), *ERAL Source-based method for solidification phase change*, Numerical Heat Transfer, Part B Fundamentals, 19(2), 175-189.
19. Jiang, S.C., Ma, N., Li, H.J., & Zhang, X.X., (2002), *Effects of thermal properties and geometrical dimensions on skin burn injuries*. Burns, 28(8), 713-717.
20. Takata, A.N., (1974), *Development of criterion for skin burns*, Aerospace Medicine, 45, 634-637.
21. Henriques Jr, F. C., & Moritz, A. R., (1947), *Studies of thermal injury: I. The conduction of heat to and through skin and the temperatures attained therein. A theoretical and an experimental investigation*, The American Journal of Pathology, 23(4), 530.
22. Henriques, F.C., (1947), *Studies of thermal injury. V. The predictability and the significance of thermally induced rate processes leading to irreversible epidermal injury*, Archives of Pathology, 43, 489-502.
23. Fugitt, C.E., (1955), *A rate process of thermal injury*, Armed Forces Special Weapons Project, AFSWP-606.
24. Stoll, A.M., & Greene, L.C., *Relationship between pain and tissue damage due to thermal radiation*. Journal of Applied Physiology, 1959, 14(3), 373-382.